# CrystEngComm

Accepted Manuscript

ROYAL SOCIETY OF CHEMISTRY

www.rsc.org/crystengcomm

Journal Name

RSCPublishing

ARTICLE

Cite this: DOI: 10.1039/x0xx00000x

# New self-assembly hybrid compounds based on arsenic-vanadium clusters and transition metal mixed-organic-ligand complexes

Hai-Yang Guo, [a] Zhi-Fang Li,[b] Xiao-Zhang,*[c] Li-Wei Fu,[a] Yang-Yang Hu,[a] Lan-Lan Guo [a] Xiao-Bing Cui*[a] Qi-Sheng Huo[a] and Ji-Qing Xu[a]

Received 00th January 2012,
Accepted 00th January 2012

DOI: 10.1039/x0xx00000x

www.rsc.org/

Seven novel compounds based on arsenic-vanadium clusters [Ni(im)(2,2’-bpy)]$_2$[Ni(im)$_2$]$_2$[Ni(2,2’-bpy)][As$_8$V$_{14}$O$_{42}$(H$_2$O)] (**1**), [Ni(2,2’-bpy)$_3$][Ni(im)$_2$]$_{0.5}$[Ni(2,2’-bpy)(im)][As$_8$V$_{14}$O$_{42}$(H$_2$O)] (**1a**), [Ni(2,2’-bpy)(phen)][Ni(2,2’-bpy)$_2$][As$_8$V$_{14}$O$_{42}$(H$_2$O)]·H$_2$O (**2**) and [Ni(2,2’-biim)(2,2’-bpy)$_2$]$_2$[As$_8$V$_{14}$O$_{42}$(H$_2$O)]·6H$_2$O (**3**) [Cd(2,2’-bpy)(phen)$_2$]$_2$[As$_8$V$_{14}$O$_{42}$(H$_2$O)]·4H$_2$O (**4**) [Cd$_4$(phen)$_4$(ox)(H$_2$O)$_6$][As$_6$V$_{15}$O$_{42}$(H$_2$O)]·2H$_2$O (**5**) [Co$_2$(phen)$_4$(ox)][H$_2$As$_8$V$_{14}$O$_{42}$(H$_2$O)]·(apy)$_2$·2H$_2$O (**6**) (Him=Imidazole, phen =1, 10-phenanthroline, 2,2’-biim=2,2’-biimidazole, apy = 2-aminopyridine) have been synthesized and characterized by IR, UV-Vis, XRD, TG, CD spectrum, elemental analysis and single-crystal X-ray diffraction analysis. Crystal analysis reveals that compound **1** is the first example of a hybrid compound constructed from polyoxometalates and transition metal mixed-organic-ligand complexes of negatively charged nitrogen-containing ligands and neutral nitrogen-containing ligands. Compound **1a** is the first example of POM supported TMCs which is formed via arsenic-metal contact. Compound **2** is a chiral compound which exhibits a novel 1-D triple-chain structure constructed from [As$_8$V$_{14}$O$_{42}$(H$_2$O)]$^{4-}$ clusters, a type of chiral transition metal mixed-organic-ligand complexes and a type of chiral transition metal complexes. Compounds **3** and **4** are supramolecular compounds which are formed by [As$_8$V$_{14}$O$_{42}$(H$_2$O)]$^{4-}$ clusters and transition metal mixed-organic-ligand complexes, respectively. Compounds **5** and **6** are constructed from arsenic-vanadium clusters and transition metal complexes of nitrogen containing ligands and oxalic groups. The catalytic properties of compounds **1** and **2-6** have been done and we found that the transition metal mixed-organic-ligand complexes have dramatically influences on the catalytic properties of catalysts.

## Introduction

Polyoxometalates (POMs) are a versatile family of molecular metal-oxygen clusters, which exhibit diverse structures and tunable properties, and have found numerous applications in analytical chemistry, materials science, magnetism, catalysis and medicine.[1] A recent major advance in the burgeoning field of the POM chemistry is that a large number of hybrid compounds constructed from the combination of POMs and transition metal complexes (TMCs) have been obtained.[2,3,4,5,6]

An intelligent choice of POMs and TMCs may give rise to materials with fascinating structures and desirable properties. The diversity of POMs and TMCs has led to a wide array of functional organic-inorganic hybrid materials. POM compounds can be directly used to prepare POM-TMC hybrids where the structural integrity of the POM can be maintained throughout construction processes or POMs in POM-TMC hybrids can be synthesized *in situ* from corresponding metal oxides. On the other hand, TMCs in POM-TMC hybrids can always be synthesized *in situ* from corresponding metal salts and corresponding organic moieties. The TMC almost always contains two parts: a central metal ion and a type of organic ligands. Thus far, it has been demonstrated that organic ligands which can be used to construct abundant TMCs play the most important role in the design and synthesis of desirable POM-TMC hybrids. The changes in the functional-group, flexibility, length, and symmetry of ligands can result in a remarkable class of POM-TMC hybrids bearing diverse architectures and functions.[2-5]

It is very common that a metal ion can be simultaneously coordinated by more than one type of organic ligands, and such compounds constitute a large and important family of coordination complexes: transition metal mixed-organic-ligand complexes (TMMCs). However, though the chemistry of hybrids of POM-TMC has developed for several decades, TMMCs, as one of the most important families of TMCs, are seldom used to prepare POM-TMC hybrids. The number of hybrids of POMs and TMMCs can almost be missed, only a few compounds based on POMs and TMMCs were reported.[7,8,9]

Table 1. Crystal data and structural refinements for compounds **1**,**1a**, **2**- **6**

| | Compound **1** | Compound **1a** | Compound **2** | Compound **3** |
|---|---|---|---|---|
| Empirical formula | $C_{48}H_{46}As_8N_{18}Ni_5O_{43}V_{14}$ | $C_{46}H_{41}As_8N_{12}Ni_{2.5}O_{43}V_{14}$ | $C_{42}H_{36}As_8N_8Ni_2O_{44}V_{14}$ | $C_{52}H_{58}As_8N_{16}Ni_2O_{49}V_{14}$ |
| Formula weight | 3169.10 | 2909.20 | 2786.73 | 3121.08 |
| Crystal system | monoclinic | Orthorhombic, | orthorombic | tetrahedral |
| space group | P2/c | P2(1)2(1)2(1) | P2(1)2(1)2(1) | I4(1)/a |
| a (Å) | 14.861(3) | 13.8011(2) | 12.169(2) | 15.565(1) |
| b (Å) | 14.142(3) | 23.8678(2) | 16.057(3) | 15.565(1) |
| c (Å) | 22.798(5) | 27.1204(2) | 40.244(8) | 38.904(5) |
| α (°) | 90 | 90 | 90 | 90 |
| β (°) | 106.37(3) | 90 | 90 | 90 |
| γ (°) | 90 | 90 | 90 | 90 |
| Volume ($Å^3$) | 4597.0(17) | 8933.50(14) | 7863(3) | 9424.8(17) |
| Z | 2 | 4 | 4 | 4 |
| $D_C$ ($Mg\cdot m^{-3}$) | 2.289 | 2.163 | 2.354 | 2.200 |
| μ ($mm^{-1}$) | 5.296 | 4.933 | 5.483 | 4.594 |
| F(000) | 3060 | 5604 | 5352 | 6064 |
| θ for data collection | 1.72 to 25.19 | 2.96 to 29.07 | 1.37 to 25.22 | 1.41 to 28.27 |
| Reflections collected | 25225 | 29903 | 44504 | 29811 |
| Reflections unique | 8118 | 19099 | 14059 | 5836 |
| R(int) | 0.0624 | 0.0297 | 0.1618 | 0.0747 |
| Completeness to θ | 98.1 | 99.2 | 99.2 | 100.0 |
| parameters | 628 | 1162 | 1041 | 296 |
| GOF on $F^2$ | 1.004 | 1.043 | 1.055 | 1.062 |
| $R^a$ [I>2σ(I)] | $R_1 = 0.0740$ | 0.0445 | $R_1 = 0.0875$ | $R_1 = 0.0843$ |
| $R^b$ (all data) | $\omega R_2 = 0.2334$ | 0.1323 | $\omega R_2 = 0.2262$ | $\omega R_2 = 0.2999$ |

| | Compound **4** | Compound **5** | Compound **6** | |
|---|---|---|---|---|
| Empirical formula | $C_{68}H_{58}As_8Cd_2N_{12}O_{47}V_{14}$ | $C_{50}H_{50}As_6Cd_4N_8O_{55}V_{15}$ | $C_{60}H_{52}As_8Co_2N_{12}O_{49}V_{14}$ | |
| Formula weight | 3332.58 | 3306.20 | 3155.51 | |
| Crystal system | triclinic | Triclinic | Triclinic | |
| space group | P-1 | P-1 | P-1 | |
| a (Å) | 11.5263(9) | 12.541(2) | 11.6254(3) | |
| b (Å) | 15.2606(11) | 12.565(2) | 14.4554(4) | |
| c (Å) | 15.8895(12) | 14.238(3) | 14.6510(4) | |
| α (°) | 106.2380(10) | 83.592(2) | 99.363(2) | |
| β (°) | 95.3720(10) | 79.184(3) | 97.293(2) | |
| γ (°) | 102.4660(10) | 81.137(2) | 91.069(2) | |
| Volume ($Å^3$) | 2584.6(3) | 2169.4(7) | 2407.70(12) | |
| Z | 1 | 1 | 1 | |
| $D_C$ ($Mg\cdot m^{-3}$) | 2.141 | 2.531 | 2.176 | |
| μ ($mm^{-1}$) | 4.237 | 4.867 | 4.449 | |
| F(000) | 1608 | 1581 | 1528 | |
| θ for data collection | 1.44 to 28.35 | 2.02 to 27.31 | 2.96 to 28.98 | |
| Reflections collected | 16505 | 13153 | 20076 | |
| Reflections unique | 12049 | 9417 | 10917 | |
| R(int) | 0.0179 | 0.0325 | 0.0273 | |
| Completeness to θ | 99.3 | 98.3 | 99.8 | |
| parameters | 745 | 653 | 736 | |
| GOF on $F^2$ | 1.073 | 1.018 | 1.024 | |
| $R^a$ [I>2σ(I)] | $R_1 = 0.0543$ | 0.0967 | $R_1 = 0.0714$ | |
| $R^b$ (all data) | $\omega R_2 = 0.1751$ | 0.2426 | $\omega R_2 = 0.2307$ | |

$^a$ $R_1 = \sum||F_0|-|F_c||/\sum|F_0|$. $^b$ $\omega R_2 = \{\sum [w (F_0^2-F_c^2)^2]/\sum[w(F_0^2)^2]\}^{1/2}$.

According to different TMMC organic ligands, compounds of POM-TMMC can be classified into three different groups: namely type **1**, type **2** and type **3**. Type **1** hybrids contains more than one type of TMMC N-containing organic ligands;[6] type **2** hybrids contain more than one type of TMMC carboxylates; type **3** hybrids contain more than one type of TMMC organic ligands being composed of both N-containing organic ones and carboxylates.[7,8]

Recently, we began the research for POM-TMMC hybrids. We have recently successfully designed and prepared some novel hybrids based on Keggin POMs and TMMCs.[5c, 10]

An important subclass of polyoxometalates is the family of arsenic-vanadium clusters derived from the well-known $\{V_{18}O_{42}\}$ cluster shell, which display interesting electronic and magnetic properties.[11] Our group has focused on the synthesis of vanadoarsenates for several years. After preparations of hybrids based on Keggin POMs and TMMCs, we begun to use $\{As_8V_{14}O_{42}(X)\}$ (X=$H_2O$, $SO_4^{2-}$ etc., $As_8V_{14}$) or $\{As_6V_{15}O_{42}(X)\}$ (X=$H_2O$, $As_6V_{15}$) to construct hybrids based on TMMCs. And fortunately, we successfully synthesized three novel compounds which are formed by $As_8V_{14}$ clusters and different TMMCs (type **1** hybrids) [Ni(im)(2,2'-

bpy)]$_2$[Ni(im)$_2$]$_2$[Ni(2,2’-bpy)][As$_8$V$_{14}$O$_{42}$(H$_2$O)] (**1**), [Ni(2,2’-bpy)$_3$][Ni(im)$_2$]$_{0.5}$[Ni(2,2’-bpy)(im)][As$_8$V$_{14}$O$_{42}$(H$_2$O)] (**1a**), [Ni(2,2’-bpy)(phen)][Ni(2,2’-bpy)$_2$][As$_8$V$_{14}$O$_{42}$(H$_2$O)]·H$_2$O (**2**) and [Ni(2,2’-biim)(2,2’-bpy)$_2$]$_2$[As$_8$V$_{14}$O$_{42}$(H$_2$O)]·6H$_2$O (**3**), [Cd(2,2’-bpy)(phen)$_2$]$_2$[As$_8$V$_{14}$O$_{42}$(H$_2$O)]·4H$_2$O (**4**) [Cd$_4$(phen)$_4$(ox)(H$_2$O)$_6$][As$_6$V$_{15}$O$_{42}$(H$_2$O)]·2H$_2$O (**5**) [Co$_2$(phen)$_4$(ox)][H$_2$As$_8$V$_{14}$O$_{42}$(H$_2$O)]·(apy)$_2$·2H$_2$O (**6**). Compound **1** is the first example of a hybrid compound constructed from POMs and TMMCs of negatively charged nitrogen-containing ligands and neutral nitrogen-containing ligands. Compound **1a** is the first example of POM supported TMCs which is formed via arsenic-metal contact. Though As-M contact Compound **2** is a chiral compound which exhibits a novel 1-D triple-chain structure constructed from As$_8$V$_{14}$ clusters, one type of chiral TMMCs and one type of chiral TMCs. Compounds **3** and **4** are supramolecular compounds which are formed by As$_8$V$_{14}$ clusters and TMMCs. It should be noted that compounds **1-4** and **1a** can be grouped as type **1** hybrids. Compounds **5** and **6** are different from compounds **1-4** and **1a**, which are constructed from arsenic-vanadium clusters and transition metal complexes of nitrogen containing ligands and oxalic groups. Compound **5** is the first example of compound formed by As$_6$V$_{15}$ clusters and TMMCs, and compound **6** is the first example of compound constructed from POMs, TMMCs and dissociated organic moieties. Compounds **5** and **6** can be groups as type **3** hybrids. The catalytic properties of compounds **1-6** have been done and we found that TMMCs have dramatically influences to the final catalytic properties of catalysts.

## Experimental

### Materials and methods

All chemicals used were of reagent grade and were used without further purification. C, H, N elemental analyses were carried out on a Perkin-Elmer 2400 CHN elemental Analyzer. Infrared spectra were recorded as KBr pellets on a Perkin-Elmer SPECTRUM ONE FTIR spectrophotometer. Inductively coupled plasma (ICP) elemental analyses were carried out on a Perkin-Elmer Optima 3300DV ICP spectrometer. UV-Vis spectra of N,N-dimethylformamide saturated solutions of compounds **1-3** were recorded on a Shimadzu UV-3100 spectrophotometer. Small-angle X-ray diffraction (XRD) patterns were obtained on a Siemens D5005 diffractometer using the Cu Kα radiation. TG curves were performed on a Perkin-Elmer TGA-7000 thermogravimetric analyzer in the flowing N$_2$ with a temperature ramp rate of 10°C min$^{-1}$. The solid state circular dichroism (CD) spectrum of compound **2** was recorded at room temperature with a Jasco J-810(S) spectropolarimeter.

### Synthetic procedures

**Synthesis of [Ni(im)(2,2’-bpy)]$_2$[Ni(im)$_2$]$_2$[Ni(2,2’-bpy)][As$_8$V$_{14}$O$_{42}$(H$_2$O)] (1) and [Ni(2,2’-bpy)$_3$][Ni(im)$_2$]$_{0.5}$[Ni(2,2’-bpy)(im)][As$_8$V$_{14}$O$_{42}$(H$_2$O)] (1a)**

Compound **1** was synthesized hydrothermally by reacting of V$_2$O$_5$ (0.350g, 2.0mmol), H$_2$C$_2$O$_4$·H$_2$O (0.470g, 3.7mmol), NaAsO$_2$ (0.332g, 2.6mmol), NiCl$_2$·6H$_2$O (0.347g, 1.46mmol), Him (0.205g, 3.0mmol), 2,2’-bpy(0.156g, 0.1mmol) and H$_2$O (20ml) was stirred for 3h, and then was sealed in a Teflon-lined stainless bomb and heated at 170ºC for 5 days. The pH of the mixture was necessarily adjusted to 5 with NH$_3$·H$_2$O solution. The mixture of black columnar crystals of compound **1** and black needle-like crystals of compound **1a** were filtered off, washed with water, and air-dried at room temperature (ca, 42.0% yield based on V). It should be noted that crystals of compound **1** are the main part of the mixture and only few crystals of compound **1a** is found in the mixture. Calcd. For C$_{48}$H$_{46}$As$_8$N$_{18}$Ni$_5$O$_{43}$V$_{14}$: As, 18.91; Ni, 9.26; V, 22.50; C, 18.19; H, 1.46; N, 7.96%. Found: As, 18.80; Ni, 9.05; V, 22.44; C, 18.11; H, 1.60; N, 7.92%. IR (cm-1): 3414, 3137, 1962, 1593,1539,1468,1440, 1312, 1257, 1238, 1156, 1094, 1074, 999, 827, 757, 715, 631, 555, 459. IR (cm$^{-1}$): 3414, 3137, 3062, 2946, 2841, 1593, 1539, 1468, 1440, 1312, 1238, 1156, 1094, 1074, 999, 827, 757, 715, 631, 555, 459. Unfortunately, for the yield of compound **1a** is very low, thus, only the ICP and IR analysis of compound **1a** were not carried out.

**Synthesis of [Ni(2,2’-bpy)(phen)][Ni(2,2’-bpy)$_2$][As$_8$V$_{14}$O$_{42}$(H$_2$O)]·H$_2$O (2)**

Compound **2** was synthesized hydrothermally by reacting of V$_2$O$_5$ (0.434g, 2.4mmol), H$_2$C$_2$O$_4$·H$_2$O (0.126g, 1.0mmol), NaAsO$_2$ (0.146g, 1.1mmol), NiCl$_2$·6H$_2$O (0.230g, 1.0mmol), phen (0.104g, 0.5mmol), 2,2’-bpy (0.104g, 0.7mmol), tartaric acid (0.204g, 1.4mmol) and H$_2$O (20ml) was stirred for 3h, and then the mixture was sealed in a Teflon-lined stainless bomb and heated at 170ºC for 5 days. The pH of the mixture was necessarily adjusted to 5 with NH$_3$·H$_2$O solution. The resulting black block crystals of compound **2** were filtered off, washed with water, and air-dried at room temperature (ca, 25.2% yield based on V). Calcd. For C$_{42}$H$_{36}$As$_8$N$_8$Ni$_2$O$_{44}$V$_{14}$: As, 21.51; Ni, 4.21; V, 25.59; C, 18.10; H, 1.30; N, 4.02%. Found: As, 21.83; Ni, 4.00; V, 25.47; C, 18.18; H, 1.55; N, 3.91%. IR (cm-1): 3452, 3052, 1675, 1601, 1518, 1473, 1445, 1426, 1344, 1314, 1248, 1148, 1106, 1005, 959, 831, 761, 711, 634, 557, 462. Compound **2** can also be prepared at pH of 4 or 6.

**Synthesis of [Ni(2,2’-biim)(2,2’-bpy)$_2$]$_2$[As$_8$V$_{14}$O$_{42}$(H$_2$O)]·6H$_2$O (3)**

Compound **3** was synthesized hydrothermally by reacting of NH$_4$VO$_3$(0.237g, 2.0mmol), H$_2$C$_2$O$_4$·H$_2$O (0.357g, 2.83mmol), NaAsO$_2$ (0.21g, 1.60mmol), NiCl$_2$·6H$_2$O (0.168 g, 0.71mmol), 2,2’-biim (0.087g, 0.065mmol), 2,2’-bpy (0.165 g, 1.0 mmol), phthalic anhydride (0.096 g, 0.65 mmol) and H$_2$O (20ml) was stirred for 0.5 h, and then was sealed in a Teflon-lined stainless bomb and heated at 160ºC for 5 days. The pH of the mixture was necessarily adjusted to 5 with NH$_3$·H$_2$O solution. The resulting black octahedron crystals of **3** were filtered off, washed with water, and air-dried at room temperature (ca, 16.5% yield based on V). Calcd. For C$_{52}$H$_{58}$As$_8$N$_{16}$Ni$_2$O$_{49}$V$_{14}$: As, 19.20; Ni, 3.76; V, 22.85; C, 20.01; H, 1.87; N, 7.18%. Found: As, 19.04; Ni, 3.56; V, 22.32; C, 20.43; H, 1.29; N, 7.32%. IR (cm-1): 3405, 3113, 3076, 2994, 2927, 2714, 1676, 1599, 1526, 1472, 1443, 1314, 1251, 1175, 1105, 1071, 997, 823, 758, 714, 554, 463. compound **3** can also be prepared by adjusting pH to 7, however, we did not obtain the product at pH value of 6.

**Synthesis of [Cd(2,2’-bpy)(phen)$_2$]$_2$[As$_8$V$_{14}$O$_{42}$(H$_2$O)]·4H$_2$O (4)**

Compound **4** was synthesized hydrothermally by reacting of V$_2$O$_5$ (0.111g, 0.6mmol), NaAsO$_2$ (0.148g, 1.1mmol), CdCl$_2$·2.5H$_2$O (0.126g, 0.6mmol), tartaric acid (0.102, 0.7mmol), phen (0.090g, 0.5mmol), 2,2’-bpy (0.108g, 0.7mmol) and H$_2$O (20ml) was stirred for 1h, and then was sealed in a Teflon-lined stainless bomb and heated at 170ºC for 5 days. The pH of the mixture was necessarily adjusted to 5 with NH$_3$·H$_2$O solution. The resulting black block crystals of **4** were filtered off, washed with water, and air-dried at room temperature (ca, 28.0% yield based on V). Calcd. For

$C_{68}H_{58}As_8Cd_2N_{12}O_{47}V_{14}$: As, 17.98; Cd, 6.75; V, 21.40; C, 24.51; H, 1.75; N, 5.04%. Found: As, 18.04; Ni, 6.60; V, 21.21; C, 24.37; H, 1.33; N, 5.29%. IR (cm-1): 3431, 3109, 1592, 1517, 1473, 1424, 1313, 1223, 1144, 1102, 995, 825, 803, 758, 717, 633, 557. Compound **4** can also be prepared with pH of 4 or 6.

**Synthesis of $[Cd_4(phen)_4(ox)(H_2O)_6][As_6V_{15}O_{42}(H_2O)]\cdot 2H_2O$ (5)**

Compound **5** was synthesized hydrothermally by reacting of $V_2O_5$ (0.163g, 0.9mmol), $H_2C_2O_4\cdot H_2O$ (0.252g, 2.0mmol), $NaAsO_2$ (0.13g, 1.0mmol), $CdBr_2\cdot 4H_2O$ (0.227g, 0.7mmol), tartaric acid (0.152, 1.0mmol), phen (0.077 g, 0.4mmol), 2,2-bpy(0.098g, 0.6mmol) and $H_2O$ (20 ml) was stirred for 1 h, and then was sealed in a Teflon-lined stainless bomb and heated at 170ºC for 5 days. The pH of the mixture was necessarily adjusted to 9 with $NH_3\cdot H_2O$ solution. The resulting black block crystals of **5** were filtered off, washed with water, and air-dried at room temperature (ca, 32.0% yield based on V). Calcd. For $C_{50}H_{50}As_6Cd_4N_8O_{55}V_{15}$: As, 13.60; Cd, 13.60; V, 23.11; C, 18.16; H, 1.52; N, 3.39%. Found: As, 13.41; Cd, 13.36; V, 22.92; C, 18.20; H, 1.42; N, 3.31%. IR (cm-1):3533, 1615, 1515, 1426, 1324, 1169, 982, 807, 726, 636, 467.

**Synthesis of $[Co_2(phen)_4(ox)][H_2As_8V_{14}O_{42}(H_2O)]\cdot(apy)_2\cdot 2H_2O$ (6)**

Compound **6** was synthesized hydrothermally by reacting of $V_2O_5$ (0.181g, 1.0mmol), $H_2C_2O_4\cdot H_2O$ (0.202 g, 1.6mmol), $NaAsO_2$ (0.34g, 2.6mmol),$CoCl_2\cdot 6H_2O$ (0.241g, 1.0mmol), phen (0.077g, 0.4mmol), 2-aminopyridine (0.094g, 1.0mmol) and $H_2O$ (20 ml) was stirred for 2h, and then was sealed in a Teflon-lined stainless bomb and heated at 170 ºC for 5 days. The pH of the mixture was necessarily adjusted to 4.5 with HCl solution. The resulting black columnar crystals of **6** were filtered off, washed with water, and air-dried at room temperature (ca, 28.0% yield based on V). Calcd. For $C_{60}H_{52}As_8Co_2N_{12}O_{49}V_{14}$: As, 18.99; Co, 3.74; V, 22.60; C, 22.84; H, 1.66; N, 5.33%. Found: As, 19.18; Co, 3.61; V, 22.44; C, 22.50; H, 1.41; N, 5.17%. IR (cm-1): 3401, 3186, 3074, 2922, 1615, 1519, 1427, 1324, 1169, 1142, 1000, 848, 828, 724, 686, 597, 460.

## Crystallography

The reflection intensity data for compounds **1-5** were measured on a Bruker Apex II diffractometer with graphite monochromated Mo $K_{\alpha}$ ($\lambda$ = 0.71073Å) radiation and the data of compound **1a** and **6** was measured on an Agilent Technology SuperNova Eos Dual system with a Mo-Kα ($\lambda$ = 0.71073Å) microfocus source and focusing multilayer mirror optics. The crystals showed no evidence of crystal decay during the data collections. Refinements were carried out with SHELXS-2014/7[12] and SHELXL-2014/7[12] using WinGX via the full matrix least-squares on $F_2$ method.[13] In the final refinements, all atoms were refined anisotropically in compounds **1-6** and **1a**. The hydrogen atoms of 2,2'-bpy, 2,2'-biim, phen, apy and $im^-$ ligands in the seven compounds were placed in calculated positions and included in the structure factor calculations but not refined, while only hydrogen atoms of part of water molecules were added. CCDC number: 1424795 for compound **1**, 1424796 for compound **1a**, 1424797 for compound **2**, and 1424798 for compound **3**, 1430182 for compound **4**, 1430183 for compound **5**, 1430184 for compound **6**, These data can be obtained free of charge via www.ccdc.cam.ac.uk/conts/retrieving.html (or from the Cambridge Crystallographic Data Centre, 12, Union Road, Cambridge CB2 1EZ, UK; Fax: (+44) 1223-336-033; or deposit@ccdc.cam.ac.uk).

## Results and discussion

**Synthesis** Compounds **1-4**, **1a** and **6** are all based on $As_8V_{14}$ clusters and compound **5** is based on $As_6V_{15}$ clusters. Our previous study on As-V clusters has demonstrated that $As_8V_{14}$ clusters are easy to be synthesized under weakly acidic conditions but $As_6V_{15}$ clusters are easy to be synthesized under weakly basic conditions.[14] The syntheses of compounds **1-6** and **1a** further confirm our previous conclusion.

Oxalic acid is important for the synthesis of compounds **1-3** and **1a**. The oxalic acid not only acts as a reducing agent but also can adjust the pH value of the reaction mixtures. The oxalic acid is especially important for the preparations of compounds **5** and **6**, in which the oxalic group was successfully introduced as a ligand coordinating to transition metal atoms. However, we have not drawn a reasonable conclusion on when and how the using of the oxalic acid can lead to preparations of similar compounds to compounds **5** and **6**.

**Structure of compound 1** Single crystal X-ray diffraction analysis reveals that the asymmetric unit of compound **1** consists of half a $[As_8V_{14}O_{42}(H_2O)]^{4-}$, one $[Ni(2,2'\text{-bpy})(im)]^{+}$, two $[Ni(im)_2]$ and half a $[Ni(2,2'\text{-bpy})]^{2+}$. $[As_8V_{14}O_{42}(H_2O)]^{4-}$ comprises 14 distorted $VO_5$ square pyramids and 8 $AsO_3$ triangular units, with a water molecule enclosed at its centre. Oxidation states of As and V were calculated using the parameters given by Brown.[15] Results indicate that vanadiums and arsenics are in the +4 and +3 oxidation states.

There are five crystallographically independent nickel ions in the asymmetric unit of compound **1** (Fig. 1a). Both Ni(1) and Ni(4) are located at special positions with occupancy factors of 0.5, whereas Ni(2) and Ni(3) are located at special positions with occupancy factors of 0.25. Ni(1) exhibits a trigonal planar geometry with two nitrogens from a 2,2'-bpy with Ni-N distances of 1.89(2)-2.07(2)Å and O(3) from $[As_8V_{14}O_{42}(H_2O)]^{4-}$ with a Ni-O distance of 1.781(9)Å. From another standpoint, $[As_8V_{14}O_{42}(H_2O)]^{4-}$ acting as an inorganic ligand via its terminal oxygen O(3) coordinates to Ni(1) to form a $As_8V_{14}$ POM supported transition metal complex.

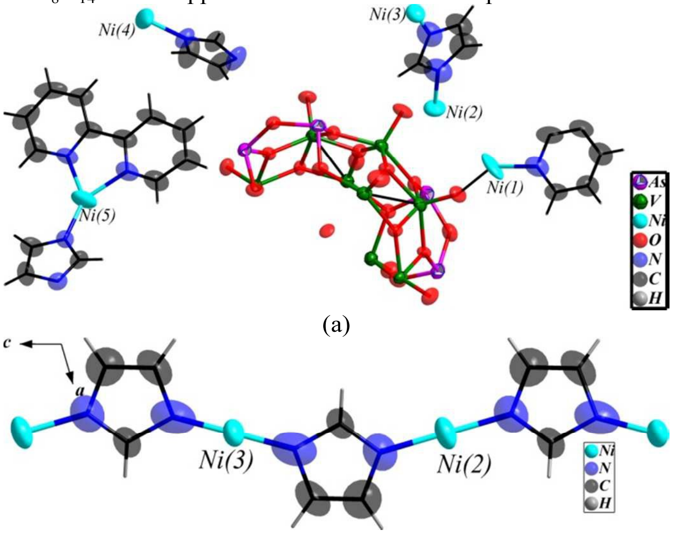

(a)

(b)

Fig. 1 (a) ball-and-stick representation of the asymmetric unit of compound **1**; (b) the pseudo-1-D chain in compound **1**.

Both Ni(2) and Ni(3) exist in linear geometries, each of which is defined by two nitrogens from two im$^-$ ligands with Ni-N distances of 1.70(2)-1.84(2)Å. N(2) im$^-$ acting as a linking agent joins Ni(2) and Ni(3) into a 1-D zigzag chain structure. However, detailed analysis found that the 1-D chain is not an actual existing one, but a disordered result of [Ni(im)$_2$] transition metal complexes. Therefore, the 1-D chain can be described as a semi-1-D chain or a pseudo-1-D chain along the *c* axis (Fig. 1b).

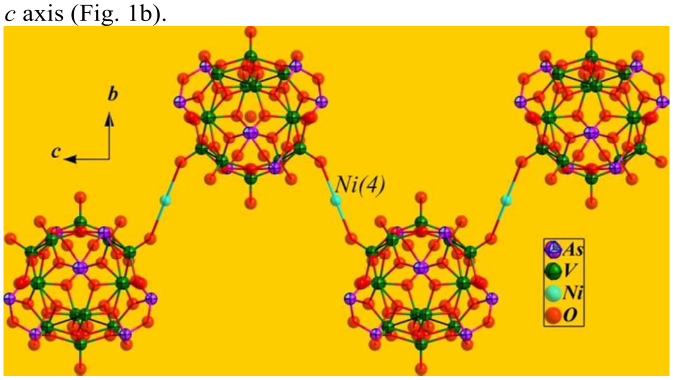

Fig. 2 the 1-D zigzag chain formed by $As_8V_{14}$ clusters and [Ni(4)(im)$_2$], carbons, nitrogens and hydrogens are omitted for clarity.

Ni(4) displays a distorted square-planar geometry involving the $N_2O_2$ donor set, where two heterocyclic nitrogens are from two im$^-$ with Ni-N distance of 1.86(1)Å and two oxygens are from two $[As_8V_{14}O_{42}(H_2O)]^{4-}$ with a Ni-O distance of 2.8552(5)Å. It should be noted that the Ni-O contacts are very weak and should be described as weak interactions. Ni(4) is coordinated not only by two im$^-$ nitrogens but also by two $As_8V_{14}$ POM oxygens, which is thoroughly different from Ni(2) and Ni(3), each of which is only bonded to two im$^-$ nitrogens. That is to say, Ni(4) leaves two free positions trans-located so that [Ni(4)(im)$_2$]$^+$ can act as a linking agent between two $[As_8V_{14}O_{42}(H_2O)]^{4-}$, via bridging oxygen atoms. Therefore, a 1-D zigzag chain was formed by the connection of one $[As_8V_{14}O_{42}(H_2O)]^{4-}$ to its two neighbours through [Ni(4)(im)$_2$] groups along the *c* axis (Fig. 2).

Ni(5) have a trigonal planar geometry too, which is coordinated by three nitrogens from a 2,2'-bpy and a im$^-$ ligands with Ni-N distances of 1.87(1)-2.02(1)Å. That is to say, Ni(5) complex is different from the other four nickel complexes, which is coordinated by two different organic ligands and should be described as a TMMC. Though the coordination spheres of Ni(5) are different from the other four, the role of the Ni(5) complex is similar to those of Ni(2) and Ni(3) complexes, which provide charge compensation for the negatively charged oxide, as well as serving as space-filling and structure-directing subunits.

In conclusion, there are five crystallographically independent nickel ions in compound **1**. Except Ni(2) and Ni(3), each of the other nickel ions plays a different role and also exhibits a different coordination sphere.

The most unusual feature of compound **1** is that there are both negatively charged nitrogen-containing ligands (im$^-$) and neutral nitrogen-containing ligands (2,2'-bpy) in its structure. All the crystallographically independent im$^-$ ligands in compound **1** are negatively charged ligands, therefore, all the Ni-N distances are in the range of 1.70(1)-1.86(1)Å, which are obviously shorter than corresponding Ni-N distances in some coordination complexes based on neutral Him ligands.[16] Some coordination complexes based on negatively charged im$^-$ were also reported previously,[17] the comparison of Ni-N distances of our compounds with the reported ones reveal that they are very similar, the comparison further confirms that the imidazole ligands in compound **1** are negatively charged ones. To the best of our knowledge, compound **1** is the first example of a hybrid compound constructed from POMs and TMMCs of negatively charged nitrogen-containing ligands and neutral nitrogen-containing ligands.

There are C-H···O hydrogen bonds in compound **1**. Carbons from [Ni(2(3))(im)$_2$] as hydrogen donors and oxygens from $[As_8V_{14}O_{42}(H_2O)]^{4-}$ as hydrogen acceptors form hydrogen bonds with C···O distances of 3.0892(6)-3.1596(7)Å. Via these C-H···O hydrogen bonds, 1-D zigzag chains in compound **1** was linked into a 3-D supramolecular structure (Fig. s1).

**Structure of compound 1a** Single crystal X-ray diffraction analysis reveals that the asymmetric unit of compound **1a** is composed of a $[As_8V_{14}O_{42}(H_2O)]^{4-}$, one [Ni(2,2'-bpy)(im)]$^{2+}$, one [Ni(2,2'-bpy)$_3$]$^{2+}$ and half a [Ni(im)$_2$]. $[As_8V_{14}O_{42}(H_2O)]^{4-}$ is identical to that of compound **1**, however, the TMCs except [Ni(im)$_2$] in compound **1a** are thoroughly different from those in compound **1**. There are three different TMCs in compound **1a**: [Ni(2,2'-bpy)$_3$]$^{2+}$, [Ni(2,2'-bpy)(im)]$^+$ and [Ni(im)$_2$]. [Ni(im)$_2$] in compound **1a** is almost identical to [Ni(im)$_2$] in compound **1** with only slight differences in bond lengths and angles. That is to say, im$^-$ of [Ni(im)$_2$] in compound **1a** is deprotonated, which is identical to that of [Ni(im)$_2$] in compound **1**. Therefore, Ni-N distances in [Ni(im)$_2$] in compound **1a** is in the range of 1.792(8)-1.79(2)Å, which are also very similar to those in [Ni(im)$_2$] in compound **1**.

At first glance, one will think that [Ni(2,2'-bpy)(im)]$^{2+}$ in compound **1a** is identical to [Ni(2,2'-bpy)(im)]$^+$ in compound **1**. However, detailed analysis found that the two are essentially different from each other. The nickel ion in [Ni(2,2'-bpy)(im)]$^{2+}$ is coordinated by a phen and a neutral im in compound **1a**, but the corresponding nickel ion in [Ni(2,2'-bpy)(im)]$^+$ is bound to a phen and a negative im$^-$ in compound **1**. The Ni-N distance between the nickel and the negative im$^-$ nitrogen is 1.87(1)Å, whereas the corresponding Ni-N distance in [Ni(2,2'-bpy)(im)]$^+$ is 1.939(9)Å, which is longer than that in compound **1**, indicating that the imidazole in [Ni(2,2'-bpy)(im)]$^{2+}$ in compound **1a** is not a deprotonated one. [Ni(2,2'-bpy)(im)]$^{2+}$ here also should be described as a TMMC.

[Ni(2,2'-bpy)$_3$]$^{2+}$ in compound **1a** displays an octahedral geometry, in which the nickel is coordinated by six nitrogens from three 2,2'-bpy ligands with Ni-N distances of 2.059(8)-2.102(9)Å. It should be noted that there is no similar TMC in compound **1** to [Ni(2,2'-bpy)$_3$]$^{2+}$ in compound **1a**.

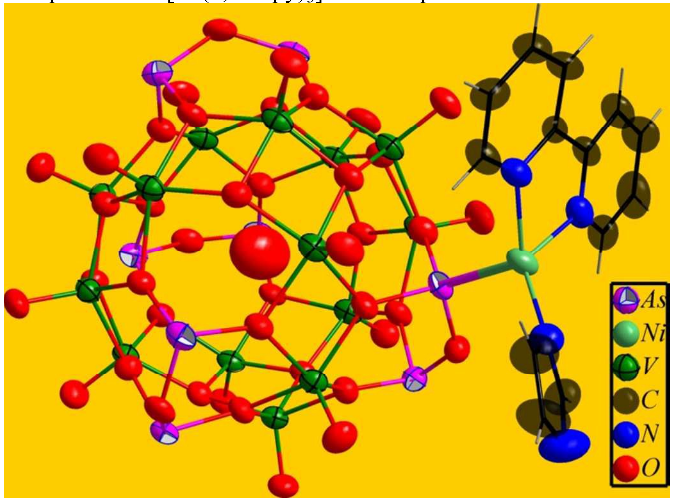

Fig. 3 ball-and-stick representation of the POM supported TMC in compound **1a**.

The most unusual feature of compound **1a** is that $[Ni(2,2'\text{-}bpy)(im)]^{2+}$ in compound **1a** is not a discrete ion, but is supported by $[As_8V_{14}O_{42}(H_2O)]^{4-}$, forming a novel POM supported TMC via a novel As-Ni contact with As-Ni distance of 2.304(2)Å, as shown in Fig. 3. It should be noted that the POM supported TMC in compound **1a** is different from the other previously reported POM supported TMCs, which are always formed via M-O contacts between M (M = transition metal, e.g. Ni) and oxygen atoms of POM clusters.[18] To the best of our knowledge, compound **1a** is the first example of POM supported TMCs which is not formed via M-O contacts. Though As-M contact (M = transition metal, e.g. Ni) is ordinarily observed in chalcogenidoarsenate compounds,[19] As-M contact has never been reported in the POM compounds before. It should be noted that the As-Ni distance is comparable to the ones in chalcogenidoarsenate compounds.

There are complex C-H···O hydrogen bonds between carbons of $[Ni(2,2'\text{-}bpy)_3]^{2+}$ and oxygens of $[As_8V_{14}O_{42}(H_2O)]^{4-}$ with C···O distances of 2.9914(0)-3.1823(0)Å, there are also multiple C-H···O hydrogen bonds between carbons of $[Ni(2,2'\text{-}bpy)(im)]^{+}$ and oxygens of $[As_8V_{14}O_{42}(H_2O)]^{4-}$ with C···O distances of 2.9679(0)-3.0856(0)Å. Except for C-H···O hydrogen bonds, there is a N-H···O hydrogen bonds between N(4) from $[Ni(2,2'\text{-}bpy)(im)]^{+}$ and O(17a, a:1+x, y, z) from $[As_8V_{14}O_{42}(H_2O)]^{4-}$ with N···O distance of 2.9857(0)Å. Via the combination of C-H···O and N-H···O hydrogen bonds, a 3-D supramolecular structure was formed (Fig. s2).

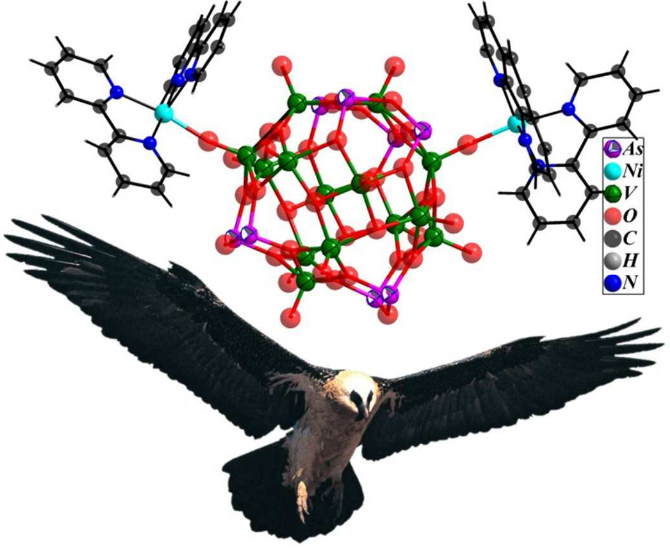

Fig. 4 ball-and-stick representation of the flying-bird-like POM bi-supported TMC in compound **2**.

**Structure of compound 2** Single crystal X-ray diffraction analysis reveals that the asymmetric unit of compound **2** is composed of a $[As_8V_{14}O_{42}(H_2O)]^{4-}$, one $[Ni(2,2'\text{-}bpy)(phen)]^{2+}$, one $[Ni(2,2'\text{-}bpy)_2]^{2+}$ and one lattice water molecule. As shown in Fig. 4, Ni(1) adopts a square pyramidal geometry and is coordinated by two nitrogens from N(5) 2,2'-bpy, two nitrogens from N(7) phen and one terminal oxygen from $[As_8V_{14}O_{42}(H_2O)]^{4-}$. Ni(2) exhibits a similar square pyramidal geometry to that around Ni(1) and is bonded to four nitrogens from two 2,2'-bpy ligands (N(1) and N(3)) and one terminal oxygen from $[As_8V_{14}O_{42}(H_2O)]^{4-}$. Ni-O and Ni-N distances are 2.03(2)-2.14(2)Å and 2.04(2)-2.10(2)Å, respectively. That is to say, $[As_8V_{14}O_{42}(H_2O)]^{4-}$ acting as a bidentate ligand coordinates to two nickel ions via its two terminal oxygen atoms to form a novel $[As_8V_{14}O_{42}(H_2O)]^{4-}$ bi-supported transition metal complex. Ni(1) and Ni(2) complexes are disposed at the two sides of $[As_8V_{14}O_{42}(H_2O)]^{4-}$, the Ni(1)-centre-Ni(2) angle is about 134º. The arrangement of Ni(1), Ni(2) complexes and $[As_8V_{14}O_{42}(H_2O)]^{4-}$ looks just like a flying bird, $[As_8V_{14}O_{42}(H_2O)]^{4-}$ is the body of the bird, and the two TMCs are the two wings of the bird (Fig. 4). The $[As_8V_{14}O_{42}(H_2O)]^{4-}$ bi-supported TMC is different from the other previously reported POM supported transition metal complexes. The two corresponding supported metal ions of each of the previously reported Keggin POM bi-supported TMCs are also located at two sides of the corresponding POM. However, those metal-centre-metal angles are about 160º, indicating that the two metal ions and the Keggin POM of the reported Keggin POM bi-supported TMCs are arranged almost linear.[18d, 20] However, the metal-centre-metal angle of compound **2** indicates that the two metal ions and $[As_8V_{14}O_{42}(H_2O)]^{4-}$ are connected to form a V-shape opening upward.

$[As_8V_{14}O_{42}(H_2O)]^{4-}$ not only coordinates to crystallographically independent $[Ni(2,2'\text{-}bpy)(phen)]^{2+}$ and $[Ni(2,2'\text{-}bpy)_2]^{2+}$, but also simultaneously coordinates to two symmetric equivalents of the two TMCs. That is to say, each $[As_8V_{14}O_{42}(H_2O)]^{4-}$ acting as a tetra-dentate ligand coordinates to four nickel complexes. Both $[Ni(2,2'\text{-}bpy)(phen)]^{2+}$ and $[Ni(2,2'\text{-}bpy)_2]^{2+}$ in compound **2** are also different from previously reported TMCs based on phen or 2,2'-bpy, it is well known that the steric hindrances of phen and 2,2'-bpy are the major influencing factor for the structures of hybrids based on phen and 2,2'-bpy for their large size, and seldom hybrids based on the linking ability of $[M(phen)_2]^{n+}$ and $[M(2,2'\text{-}bpy)_2]^{n+}$ (M=metal) were reported previously for the steric hindrances of phen and 2,2'-bpy. To the best of our knowledge, there is one compound which is based on Keggin POMs linked by $[M(2,2'\text{-}bpy)_2]^{n+}$ reported by Liu et al.[21] Detailed analysis reveals that POMs of the Liu's compound are not only connected by $[M(2,2'\text{-}bpy)_2]^{n+}$ but also are connected by $[M(en)_2]^{n+}$ (en = ethylendiamine) with minor steric hindrance.

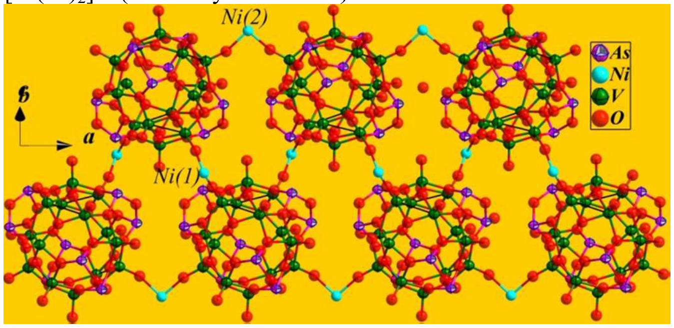

Fig. 5 the 1-D triple-chain structure formed by $As_8V_{14}$ POMs and TMCs, carbons and nitrogens are omitted for clarity.

Both $[Ni(2,2'\text{-}bpy)(phen)]^{+}$ and $[Ni(2,2'\text{-}bpy)_2]^{2+}$ in compound **2** exhibit very strong linking ability to their neighbouring $As_8V_{14}$ POMs via strong Cu-O covalent contacts. Each TMC joins two $[As_8V_{14}O_{42}(H_2O)]^{4-}$ acting as a $\mu_2$ bridge, and each $[As_8V_{14}O_{42}(H_2O)]^{4-}$ links four TMCs acting as a $\mu_4$ bridge. Therefore, the two kinds of TMCs and POMs are connected into a novel 1-D triple-chain structure. The chain structure is very interesting, as shown in Fig. 5, consisting of three chains in it, two of which are linear chain structures constructed from Ni(2) and its neighbouring POMs. Ni(2) metal centres are arranged into a linear array, and POMs are arranged into a linear array too, the line that penetrating all the Ni(2) metal centres is tangent to the surfaces of all their neighbouring POMs. The third chain in the triple-chain are more interesting, which is a right-handed helical chain constructed from Ni(1) ions and its neighbouring POMs. To the best of our knowledge, such a novel triple-chain has never been reported before.

The comparison of Ni-O distances in compound **2** with M-O distances in Liu's compound reveals that Ni-O distances of our compound are comparable to those in Liu's compound.[21] It should be noted that the steric hindrance of $[Ni(2,2'\text{-}bpy)_2]^{2+}$ in our compound should be comparable to that of Liu's compound, and the steric hindrance of $[Ni(2,2'\text{-}bpy)(phen)]^{2+}$ should be even stronger than that of Liu's compound. Therefore, the steric hindrance between TMCs and POMs in our compound did not influence Ni-O distances at all. The TMCs and POMs are stacked tightly.

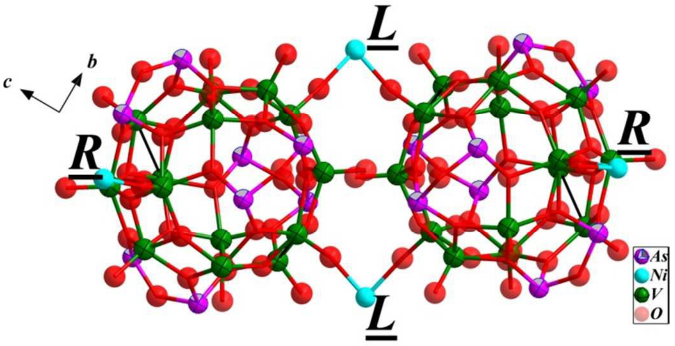

Fig. 6 ball-and-stick representation of the side-view of the 1-D triple-chain structure in compound **2** running along the a axis, carbons and nitrogens are omitted for clarity.

It should be noted that both $[Ni(2,2'\text{-}bpy)(phen)]^{2+}$ and $[Ni(2,2'\text{-}bpy)_2]^{2+}$ in compound **2** are chiral. $[Ni(2,2'\text{-}bpy)(phen)]^{2+}$ have the right handed screw (Δ) configuration, whereas $[Ni(2,2'\text{-}bpy)_2]^{2+}$ have the left handed screw (Λ) configuration. That is to say, all the Ni(2) complexes in the two linear chain structures of the 1-D triple-chain have the right handed screw (Δ) configuration, and all the Ni(1) complexes in the right-handed helical chain of the 1-D triple-chain have the left handed screw (Λ) configuration (Fig. 6). All the nickel centres in the 1-D triple-chain of compound **2** extend to the outside of the area of the cross section of the triple-chain, and the POMs are on the inside of the cross section of the triple-chain. In another word, POMs of the 1-D triple chain is fully wrapped by two different chiral TMCs arranged in four different rows as shown in Fig. 6.

There are strong intermolecular C-H···O hydrogen bonding interactions between TMC (TMMC) carbons and POM oxygens from different 1-D triple chains with C···O distances in the range of 2.9792(4)-3.1887(5)Å. A novel 3-D supramolecular structure was formed via the C-H···O hydrogen bonding interactions, as shown in Fig. s3.

**Structure of compound 3** After synthesizing compound **2**, we tried to replace phen with 2, 2'-biim to synthesize some similar compounds, for 2,2'-biim containing four coordinating nitrogen donors, which may act as a bridging ligand, however, the TMMC was successfully formed just like that in compound **2**, and 2,2'-biim did not acted as a bridge.

Single crystal X-ray diffraction analysis reveals that the asymmetric unit of compound **3** is comprised of one quarter of a $[As_8V_{14}O_{42}(H_2O)]^{4-}$, half a $[Ni(2,2'\text{-}bpy)_2(2,2'\text{-}biim)]^{2+}$ TMMC and one and a half of lattice water molecules. Ni(1) is located at a special position with occupancy factor of 0.5. The coordination sphere around Ni(1) is a distorted octahedron, in which Ni(1) is bound to six nitrogen atoms from two 2,2'-bpy and one 2,2'-biim with Ni-N distances in the range of 2.016(7)-2.10(1)Å. Both the two 2,2'-bpy coordinating to Ni(1) are twisted with a dihedral angle of 5.903º, whereas the 2,2'-biim is twisted with a dihedral angle of 7.242º. Two 2,2'-bpy ligands and one 2,2'-biim ligand chelate Ni(1) in N, N-chelating modes, forming a chiral nickel complex having right handed screw (Δ) configuration.

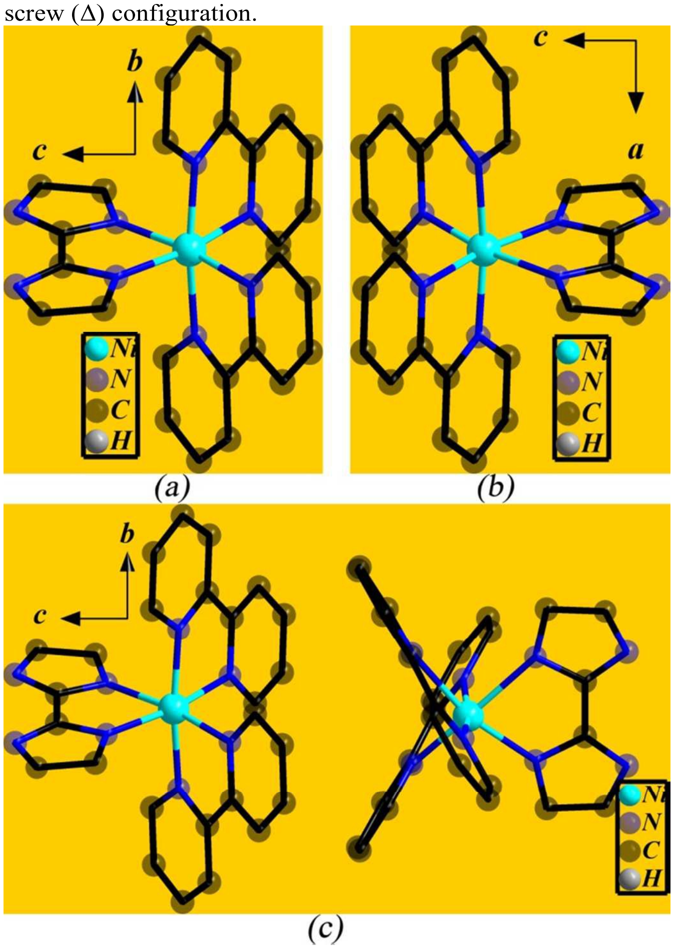

(a) (b)

(c)

Fig. 7 (a) ball-and-stick representation of the right handed screw (Δ) configuration TMC; (b) ball-and-stick representation of the left handed screw (Λ) configuration TMC; (c) ball-and-stick representation of the meso-meso dimer in compound **3**.

It should be noted that each two $[Ni(2,2'\text{-}bpy)(2,2'\text{-}biim)]^{2+}$ are arranged into a dimer with metal-metal distances of 7.0243(9)Å (Fig. 7c). One $[Ni(2,2'\text{-}bpy)_2(2,2'\text{-}biim)]^{+}$ of the dimer has the right handed screw (Δ) configuration (Fig 7a), whereas the other has the left handed screw (Λ) configuration (Fig 7b), indicating that the two are meso isomers or enantiomers of each other. That is to say, the dimer is a meso-meso dimer.

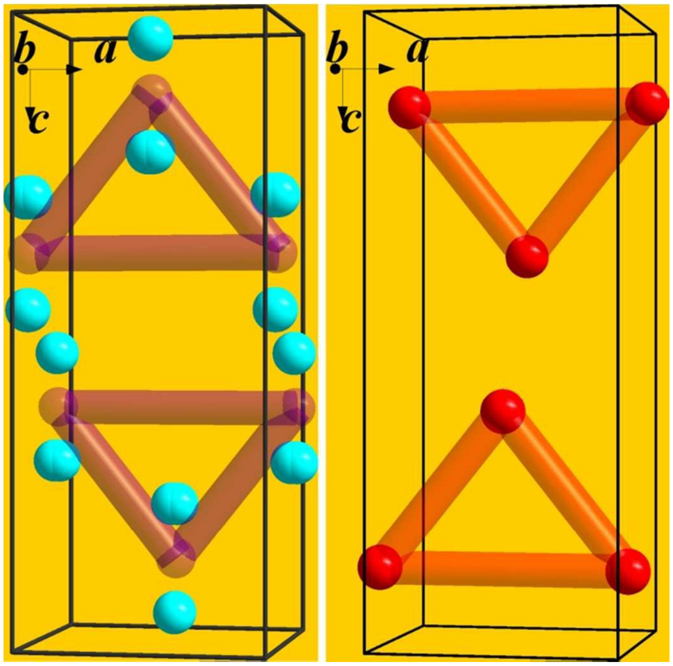

(a) (b)

Fig. 8 schematic representation of packing structures of TMCs (a) and POMs (b) in compound **3**.

There are six $As_8V_{14}$ clusters in each cell of compound **3**. The six clusters can be grouped into two sets, in each of which three clusters can be arranged into an isosceles triangle. The side length of the isosceles triangle is 12.456(1)Å, whereas the based length is 15.565(1)Å. That is to say, there are two equivalent isosceles triangles in each cell. It should be noted that the planes defined by the two isosceles triangles are parallel to each other and the base to apex directions of the two isosceles triangles are opposite to each other.

It should be noted that there also are six meso-meso dimers in each cell of compound **3**, and the six dimers can be arranged into two equivalent isosceles triangles too with side length of 12.456(1)Å and base length of 15.565(1)Å. Notably, the isosceles triangles formed by dimers are almost identical to those formed by $As_8V_{14}$ clusters. There are also two equivalent triangles in each cell, the planes defined by the two are parallel to each other and the base to apex directions of the two are opposite to each other.

The arrangement of meso-meso dimer triangles and POM triangles are also interesting. As shown in Fig. 8, the meso-meso dimer triangles and POM triangles are stacked alternately along the b axis, and the two triangles are also stacked alternately along the c axis. It should be noted that the arrangement are directed by C-H···O hydrogen bonding interactions with C···O distances of 2.8147(2)-2.9966(2)Å.

**Structure of compound 4** compound **4** is constructed from $[As_8V_{14}O_{42}(H_2O)]^{4-}$ and $[Cd(2,2'\text{-bpy})(phen)_2]^{2+}$ TMMCs. The POM in compound **4** is identical to that of compound **3**. The TMMC in compound **4** is formed by a cadmium ion chelated by two phen and a 2,2'-bpy ligands with Cd-N distances in the range of 2.328(5)-2.394(5)Å. Though both the metal centre and the organic ligands of the TMMC in compound **4** are different from those of compound **3**, the TMMCs in compounds **4** and **3** can be grouped into one type, in which its metal centre is coordinated by two types of chelating ligands: the number of one type of ligand is two, and the number of the other type of ligand is one.

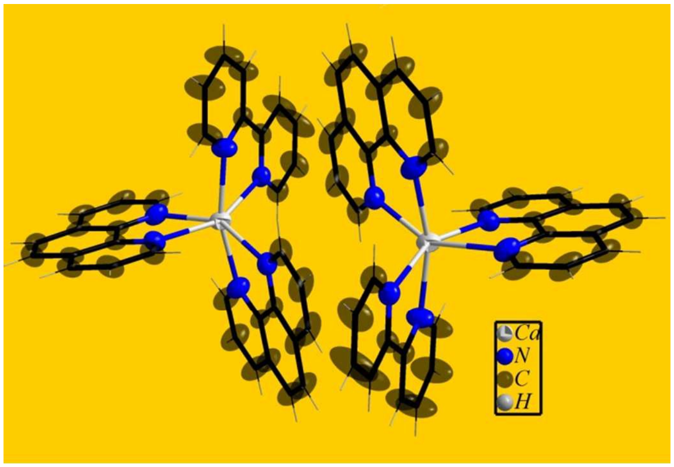

Fig. 9. Ball-and-stick representation of the meso-meso dimer in compound **4**. The right handed screw (Δ) configuration TMC is at the right, and the left handed screw (Λ) configuration TMC is at the left.

The crystallographically independent $[Cd(2,2'\text{-bpy})(phen)_2]^{2+}$ in compound **4** is also a chiral complex having right handed screw (Δ) configuration just like the TMMC in compound **3**.

Each two $[Cd(2,2'\text{-bpy})(phen)_2]^{2+}$ in compound **4** are arranged into a dimer with metal-metal distances of 7.6840(3)Å (Fig. 9). One $[Ni(2,2'\text{-bpy})_2(2,2'\text{-biim})]^{+}$ of the dimer has the right handed screw (Δ) configuration (Fig. 9), whereas the other has the left handed screw (Λ) configuration (Fig. 9). It should be noted that the dimer in compound **4** is very similar to that of compound **3**.

Though the two building blocks of compounds **3** and **4** belong to the same type, the packing structures of compounds **3** and **4** are thoroughly different from each other. The POMs in compound **4** are arranged in a row running along the a axis, whereas the dimer in compound **4** are also arranged in a row running along the a axis (Fig. s4). There also are complex C-H···O hydrogen bonding interactions in compound **4**, C···O distances are in the range of 3.0418(1)-3.1940(2)Å.

**Structure of compound 5** Single-crystal X-ray diffraction analysis reveals that $[As_6V_{15}O_{42}(H_2O)]^{4-}$ in compound **5** consists of 15 distorted $VO_5$ square pyramids and 6 $AsO_3$ triangular units, with a $H_2O$ enclosed at its centre. $[As_6V_{15}O_{42}(H_2O)]^{4-}$ in compound **5** is similar to $As_6V_{15}$ reported previously by A. Müller et al.[11a] Bond distances of our anion are comparable to those of Müller's anion. Bond valence sum calculations suggest that the arsenic atoms and the vanadium atoms are respectively in the +3 and +4 oxidation states.[15]

Compound **5** crystallizes in triclinic space group P-1. The asymmetric unit contains half a $[As_6V_{15}O_{42}(H_2O)]^{6-}$, two Cd(II) centres, two Phen ligands, half an oxalic group, three coordinated water molecules and one lattice water molecule. Cd(1) is seven-coordinated by two carboxylate oxygens, two coordinated water molecules, one terminal oxygen from $[As_6V_{15}O_{42}(H_2O)]^{6-}$ and two nitrogens from a phen ligand, generating a distorted irregular decahedron geometry (Fig. 10). Cd(2) adopts a similar irregular decahedron geometry to that of Cd(1), in which Cd(2) is seven-coordinated by one carboxylate oxygen, one coordinated water molecule, two terminal oxygen from two $[As_6V_{15}O_{42}(H_2O)]^{6-}$, and two nitrogens from a phen. The difference of the two Cd geometries is that Cd(1) is linked to only one $[As_6V_{15}O_{42}(H_2O)]^{6-}$ but Cd(2) is linked to two $[As_6V_{15}O_{42}(H_2O)]^{6-}$ serving as a $\mu_2$ bridge. Cd-O distances and Cd-N distances are in the range of 2.23(1)-2.57(1)Å and 2.35(1)-2.39(1)Å, respectively.

It is interesting to compare the cadmium coordination spheres in TMMCs of compounds **4** and **5**, the cadmium in compound **4** is only six-coordinated, whereas the cadmium in compound **5** is seven-coordinated. The reason could be ascribed to the different steric hindrances from different ligands. The phen and 2,2-bpy ligands in compound **4** have higher steric hindrances than the oxalic group and coordinated water molecules in compound **5**, indicating that more ligands like water molecules can be placed around the cadmium centre in compound **5**.

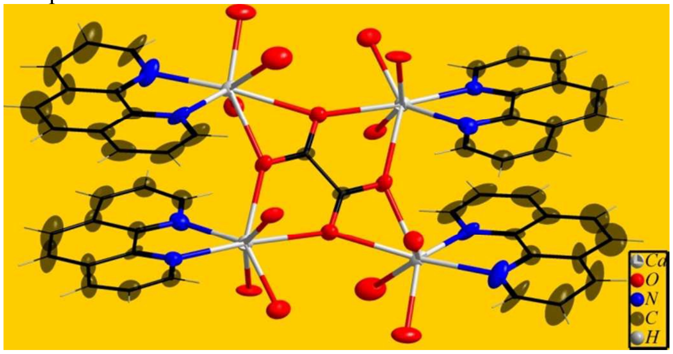

Fig. 10. Ball-and-stick representation of the TMMC in compound **5**.

The most interesting feature of the TMMC is the special coordination mode of the oxalic group. The two carboxylate groups of the oxalic group form two four-member chelate rings with two Cd(1) centres, and simultaneously, each two oxygens from two different carboxylate groups of the oxalic group form a five-member chelate ring with a Cd(2) centre. That is to say, each carboxylate group of the oxalic group adopts the same bidentate $\mu_3$ coordination mode. Therefore, the whole oxalic group acting as a $\mu_4$-bridge interacting with four cadmium ions via its four carboxylate oxygens, forming two four-member and two five-member chelate rings. Each of the four Cd centres around the oxalic group is also chelated by one phen ligand, thus, a novel transition metal mixed-organic ligand coordination complex is formed, as shown in Fig. 10. After a search of the CCDC database, we found that such a novel coordination mode of the oxalic group has never been reported before. The Cd-Cd distances of the four-cadmium-TMMC is in the range of 4.5407(7)-4.9890(9)Å.

The four-cadmium-TMMC is not discrete, but interacting with $[As_6V_{15}O_{42}(H_2O)]^{6-}$ via strong Cd-O contacts. Each Cd(1) of the TMMC joins two $[As_6V_{15}O_{42}(H_2O)]^{6-}$ with Cd-O contacts, whereas each Cd(2) only interacts with one $[As_6V_{15}O_{42}(H_2O)]^{6-}$ with Cd-O contact. That is to say, each TMMC connects four $[As_6V_{15}O_{42}(H_2O)]^{6-}$. On the other hand, each $[As_6V_{15}O_{42}(H_2O)]^{6-}$ joins four TMMCs via Cd-O contacts. Thus, a novel 2-D layer structure constructed from $[As_6V_{15}O_{42}(H_2O)]^{6-}$ and TMMCs are formed along the ab plane.

It should be noted that there are strong π···π interactions in compound **5**. The interplane distance between the two crystallographically independent phen ligands is about 3.5Å, indicating that there is strong intermolecular π···π interaction in the TMMC of compound **5**. For each TMMC is surrounded by four $[As_6V_{15}O_{42}(H_2O)]^{6-}$, indicating that there are no intermolecular π···π interaction among different TMMC phen ligands from the same 2-D layer. However, there are intermolecular π···π interactions between TMMC phen ligands from neighbouring 2-D layer structures with interplane distance of about 3.5Å. Thus, 2-D layers are stacked via intermolecular π···π interactions into a novel 3-D supramolecular structure (Fig. s5).

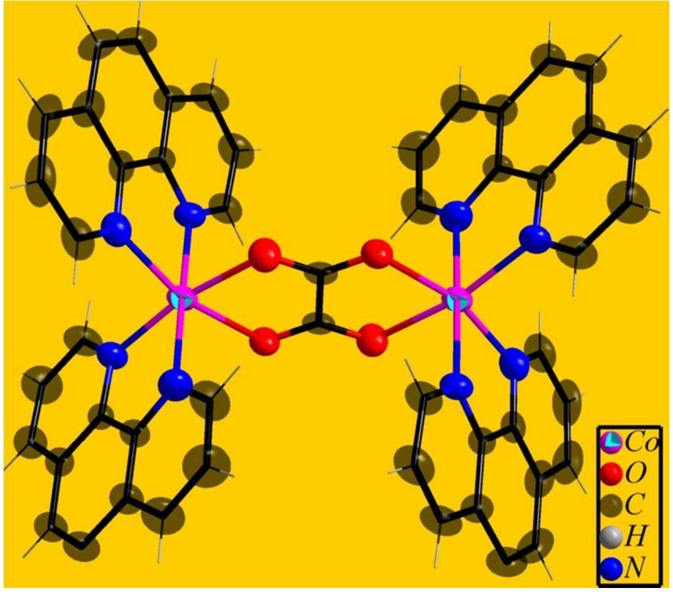

Fig. 11. Ball-and-stick representation of the TMMC in compound **6**.

**Structure of compound 6** compared with compound **5**, compound **6** is constructed from $[H_2As_8V_{14}O_{42}(H_2O)]^{2-}$, $[Co_2(phen)_4(C_2O_4)]^{2+}$ and dissociated apy molecules. The TMMC in compound **6** is also formed by phen and oxalic group but different metal center; however, the final structure of the TMMC in compound **6** is thoroughly different from that of compound **5**. Co(1) adopts an octahedral geometry with four nitrogens from two phen ligands and two oxygens from the oxalic group with Co-N and Co-O distances of 2.109(7)-2.143(7)Å and 2.117(7)-2.147(7)Å. Being different from the novel coordination mode of oxalic group in compound **5**, the oxalic group in compound **6** adopts only a bis-bidentate chelating mode coordinating to two Co(1) ions. Thus, the oxalic group acts as a $\mu_2$ bridge linking to $[Co(phen)_2]^{2+}$ into a TMMC, as shown in Fig. 11. It should be noted that such a coordination mode of oxalic group has been observed by J. M. Gutiérrez-Zorrilla and L. Lezama et al,[8c] though the TMMC in compound **6** is thoroughly different from that reported by J. M. Gutiérrez-Zorrilla and L. Lezama.[8c]

The most unusual feature of compound **6** is that it not only contains POMs and TMMCs but also contains dissociated apy moieties. Thus compound **6** is an example of a multi-component system which is more complex than the system to which compounds **1-5** belong. To the best of our knowledge, such a multi-component compound has never been reported before.

There are complex C-H···O hydrogen bonding interactions between phen carbons and terminal oxygens from $[H_2As_8V_{14}O_{42}(H_2O)]^{2-}$ with C···O distances of 2.9159(1)-3.0476(1)Å. It should be noted that the dissociated apy moieties in compound **6** are disordered, the distances of disordered nitrogens of apy molecules and oxygens from $[H_2As_8V_{14}O_{42}(H_2O)]^{2-}$ is 2.8004(1)-2.9858(1)Å.

Except for C-H···O and N-H···O and hydrogen bonding interactions, there are also π···π interactions between phenol rings of apy molecules and phen ligand from TMMCs in compound **6** with interplane distance of about 3.5Å. Thus, a 3-D supramolecular structure was formed via the combination of C-H···O, N-H···O and π···π interactions (Fig. s6).

## Characterization

In the IR spectrum of compound **1** (Fig. s7), The band at 999cm$^{-1}$ is associated with the terminal V=O stretching vibration, and strong features at 827cm$^{-1}$ and 715cm$^{-1}$ are ascribed to υ(O-V-O). The patterns of bands in the region characteristic of υ(V=O$_t$) indicate the presence of V$^{IV}$ sites: clusters which contain exclusively V$^{IV}$ generally possess υ(V=O$_t$) bands in the range of 970-1000cm$^{-1}$, while bands in the region 940-960cm$^{-1}$ are characteristic of V$^{V}$. The observation of a strong absorbance in the 970-1000cm$^{-1}$ region provides a useful diagnostic for the presence of V$^{IV}$ centres.[22] The band at 757cm$^{-1}$ corresponds to the υ(As-O) vibration. The multiple strong features in the 1238-1675cm$^{-1}$ region of the IR spectrum of compound **1** are due to vibrations of im$^-$ and phen ligands in compound **1**.

Compounds **1-4** and **6** are all based on $[As_8V_{14}O_{42}(H_2O)]^{4-}$ anions. Thus, compounds **2-4** and **6** display similar IR spectrum features to that of compound **1** with slight differences. The IR spectra of compounds **2-4** and **6** (Fig. s7) show the peaks at 1005cm$^{-1}$, 997cm$^{-1}$, 995cm$^{-1}$ and 1000cm$^{-1}$ corresponding to υ(V=O$_t$). 831cm$^{-1}$, 711 cm$^{-1}$ for compound **2**, 823cm$^{-1}$, 714cm$^{-1}$ for compound **3**, 825cm$^{-1}$, 717cm$^{-1}$ for compound **4**, and 828cm$^{-1}$ and 724cm$^{-1}$ for compound **6** are respectively due to υ(O-V-O). The bands at 761cm$^{-1}$, 758cm$^{-1}$, and 758cm$^{-1}$ corresponds to υ(As-O) of compounds **2-4**. However, the band corresponding to υ(As-O) of compound **6** was not observed. In addition, bands in the 1248-1675cm$^{-1}$, 1251-1676cm$^{-1}$, 1223-1592cm$^{-1}$ and 1142-1615cm$^{-1}$ regions of the IR spectra of compounds **2-4** and **6** are respectively due to vibrations of im and 2,2'-bpy in compound **2**, 2,2'-bpy and 2,2'-biim in compound **3**, 2,2'-bpy and phen in compounds **4** and phen, apy and oxalic group in compound **6**.

Though the POM in compound **5** is different from POMs from the other compounds, however, the IR spectrum of compound **5** is similar to those IR spectra of the other compounds. 982cm$^{-1}$ in the IR spectrum can be due to υ(V=O$_t$), whereas 807 and 726cm$^{-1}$ can be ascribed to υ(O-V-O). The characteristic peak of υ(As-O) was not observed. 1169-1615cm$^{-1}$ are due to phen and oxalic group in compound **5**.

The powder X-ray diffraction patterns for compounds **1-6** are all in good agreement with the ones simulated based on the data of the single-crystal structures, respectively, indicating the purity of the as-synthesized products (Fig. s8). The differences in reflection intensity are probably due to preferential orientations in the powder samples of compounds **1-6**.

The UV-Vis spectra of compounds **1-3,** in the range of 250-600nm, are presented in Fig. s9. The UV-Vis spectrum of compound **1** displays an intense absorption peak cantered at about 256nm assigned to an O→V charge transfer, an intense absorption peak at 303nm and an absorption shoulder at 314nm should be ascribed to $n \rightarrow \pi^*$ transitions of im$^-$ and 2,2'-bpy ligands in compound **1**. The UV-Vis spectrum of compound **2** displays an intense absorption peak at about 275nm assigned to the O→V charge transfer in the polyoxoanion structure.[23] The UV spectrum of compound **2** also exhibits two absorption shoulder peaks at about 296 and 310nm due to the $n \rightarrow \pi^*$ transitions of phen and 2,2'-bpy ligands in compound **2**. The UV-Vis spectrum of compound **3** presents strong peaks at 256 and 275nm ascribed to the O→V charge transfer in compound **3**. The UV-Vis spectrum of compounds **3** also shows strong peaks at 283, 296 and 308nm corresponding to $n \rightarrow \pi^*$ transitions of organic ligands in it. The UV-Vis spectra of compounds **4-6** are similar, each of which only exhibits a strong peak cantered at 271nm for compound **4**, 266nm for compound **5** and 268nm for compound **6**, respectively. It should be noted that the shoulder peaks of compounds **4-6** are all unobvious, the reason is that the organic ligands in compounds **4-6** are different from those in compounds **1-3**.

The TG curve of compound **1** (Fig. s10) can be divided into two stages, the first stage is from room temperature to 495°C with a weight loss of 13.1%, which is due to the release of the crystallization water molecules and negatively charged im$^-$ ligands in compound **1** (calculated: 14.0%). The second stage is from 495 to 890°C with a weight loss of 38.4%, which is ascribed to the release of 2,2'-bpy and the sublimation of $As_2O_3$ in compound **1**. The total weight loss of the TG curve is 51.5%, which is well consistent with the calculated result 53.0%. It is very interesting to observe that the TG curve of compound **1** exhibits a two-step weight loss which is consistent with the releases of im$^-$ and 2,2'-bpy respectively.

Table 2 Catalytic activity and product distribution

| Entry | Catalysts | Styrene conversion (%) | Product selectivity (%) | | |
|---|---|---|---|---|---|
| | | | so | bzdh | others |
| 1 | No catalyst | ≈ 0 | | | |
| 2 | Compound **1** | 91.8 | 90.9 | 9.1 | 0 |
| 3 | Compound **2** | >99 | 21.2 | 69.1 | 9.7 |
| 4 | Compound **3** | 54.9 | 43.8 | 56.2 | 0 |
| 5 | Compound **4** | 96.2 | 9.6 | 82.3 | 8.1 |
| 6 | Compound **5** | 58.7 | 62.4 | 37.6 | 0 |
| 7 | Compound **6** | 69.0 | 59.2 | 38.3 | 2.5 |
| 8 | Compound **7** | 48.1 | 51.5 | 48.5 | 0 |
| 9 | Compound **8** | 83.1 | 23.1 | 76.9 | 0 |

so = styrene oxide; bzdh = benzaldehyde. Compound **7** = $[As_8V_{14}O_{42}(H_2O)][Cd(1,10\text{-}Phen)_3]_2$,[24] Compound **8** = $[As_8V_{14}O_{42}(H_2O)][Ni(2,2'\text{-}biim)_3]_2\cdot 6H_2O$,[**5d**]

The epoxidation of styrene to styrene oxide with aqueous tertbutyl hydroperoxide (TBHP) using compounds **1**, **2, 3, 4, 5** or **6** as a catalyst was carried out in a batch reactor. In a typical run, the catalyst (compound **1** (10mg, 3.5μmol), compound **2** (10mg, 3.0μmol), compound **3** (10mg, 3.0μmol), compound **4** (10mg, 3.0μmol), compound **5** (10mg, 3.0μmol) compound **6** (10mg, 3.2μmol), 0.114ml (1 mmol) of styrene and 1 ml of $CH_3CN$ were added to a 10 ml two-neck flask equipped with a stirrer and a reflux condenser. The mixture was heated to 80°C and then 2 mmol of TBHP was injected into the solution to start the reaction. The liquid organic products were quantified by using a gas chromatograph (Shimadzu, GC-8A) equipped with a flame detector and an HP-5 capillary column and identified by a comparison with authentic samples and GC-MS coupling. The activity of the reaction system to oxidize styrene to styrene oxide in the absence of the catalysts was determined. The result showed that no conversion of the styrene after 8 h.

Table 2 shows the reaction results of TBHP oxidation of styrene over various catalysts at 80ºC. As expected, all the catalysts are active for the TBHP oxidation of styrene. Compound **1** catalyst shows an activity with 91.8% conversion and 90.9% selectivity to styrene oxide after 8h. Compound **2** shows a higher activity with 99% conversion of styrene and 21.2% selectivity to styrene oxide. Nevertheless, compound **3** shows a lower activity with 54.9% conversion of styrene and 43.8% selectivity to styrene oxide. The activity of compound **4** is also high with 96.8% conversion and the selectivity of compound **4** is only 9.6%. Both the activity and selectivity of compounds **5** and **6** are comparable to each other: 58.7% and 69.0% conversions for compounds **5** and **6** and 62.4% and 59.2% selectivity for compounds **5** and **6**, respectively.

We have already carried out identical catalytic experiments previously by using some similar compounds including compounds **7** and **8** as catalysts, and from those experiments we found that transition metal elements in TMCs are essentially important for the catalytic properties of catalysts used and the structures of TMCs in catalysts used also have fatal effects on their catalytic activities.[5d]

Table 3 comparisons of compounds **3**, **8** and compounds **4**, **7**.

| Compound | **3** | **8** | **4** | **7** |
|---|---|---|---|---|
| Space group | I4(1)/a | I4(1)/a | P-1 | P-1 |
| POM | $As_8V_{14}$ | $As_8V_{14}$ | $As_8V_{14}$ | $As_8V_{14}$ |
| TMC metal | Ni | Ni | Cd | Cd |
| TMC ligand | Biim,<br>2,2'-bpy | biim | Phen,<br>2,2'-bpy | phen |
| Conversion (%) | 54.9 | 83.1 | 96.2 | 48.1 |

X-ray structure analysis reveals that compounds **3** and **8** are very similar to each other, both of which are constructed from $As_8V_{14}$ POMs and $Ni(L)_3$ (L = 2,2'-bpy or 2,2'-biim) TMCs. Detailed analysis indicates that compounds **3** and **8** are almost isomorphous and isostructural to each other, the only difference of the two is two 2,2'-bpy of the TMC in compound **3** replacing two 2,2'-biim of the TMC in compound **8**. Thus, the difference of the catalytic properties of the two is mainly due to the difference of the two TMCs in compounds **3** and **8**. It is obvious that the steric hindrance of 2,2'-bpy in compound **3** is stronger than that of 2,2'-biim in compound **8**, indicating that the nickel centre in compound **3** is easier to be attacked by the styrene than that in compound **8**. Unfortunately, why 2,2'-biim or 2,2'-bpy has such a strong influence on the catalytic results of compounds **3** or **8** is still elusive.

Interestingly, the relationship between compounds **4** and **7** is very similar to that between compounds **3** and **8**. The only difference of compounds **4** and **7** is one 2,2'-bpy of the TMC in compound **4** replacing one phen of the TMC in compound **7**. Also very interestingly, the catalytic activity of compound **4** is far higher than that of compound **7**, though the difference between the steric hindrances of 2,2'-bpy and phen looks not so large. In conclusion, the introduction of TMMCs can dramatically influence the catalytic activities of catalysts: sometimes can increase the catalytic activity (compound **7** to compound **4**), and sometimes can decrease the catalytic activity (compound **8** to compound **3**). The comparisons of compounds **3**, **8** and compounds **4**, **7** are listed in Table 3. Unfortunately, the mechanism is still elusive.

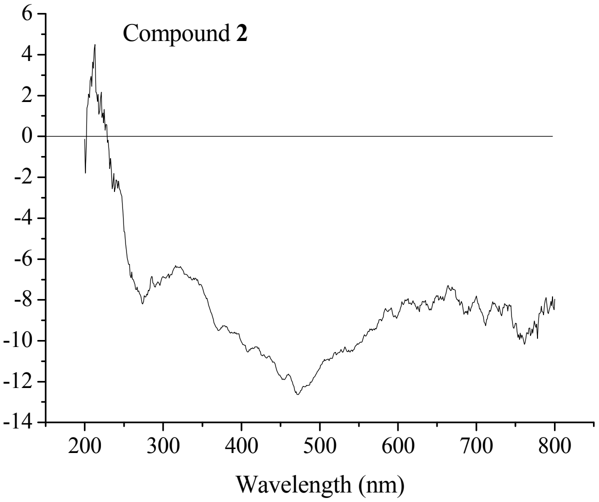

Fig. 12. Solid state CD spectrum of compound **2** as KCl pellet at room temperature.

The catalytic activities of compounds **5** and **6** are comparable, though the two are based on different metal centres. The catalytic activity of compound **1** is also high (91.8%), strangely, the catalytic activity of compound **2** is the highest one (>99%) of the eight compounds. The high catalytic activity of compound **2** perhaps can be owing to its special structure. Most importantly, compound **2** crystalizes in a chiral space group $P2_12_12_1$ and all the TMCs in compound **2** are chiral too. To explore the chirality of compound **2**, the solid-stated CD spectrum of compound **2** has been recorded. As shown in Fig. 12, the solid-state CD spectrum of compound **2** shows a broad negative cotton effect, indicating the chirality of compound **2**.

## Conclusions

seven new self-assembly hybrid compounds based on $As_8V_{14}$ and $As_6V_{15}$ clusters and transition metal mixed-organic-ligand complexes have been synthesized and characterized. Compounds **1-4** are based on As-V POMs and TMMCs of two different nitrogen-containing ligands, whereas compounds **5-6** are based on As-V POMs and TMMCs of oxalic groups and nitrogen-containing ligands. A multi-component system based on As-V POMs and TMMCs has never been systematically studied before. It should be noted that the synthesis of multi-component compounds is still a great challenge for chemists. The introduction of TMMCs to As-V POMs will increase the variety of crystal structures and crystal properties. The catalytic properties of compounds **1-6** have been done and we found that the transition metal mixed-organic-ligand complexes have dramatically influences to the catalytic properties of the compounds.

## Acknowledgements

This work was supported by National Natural Science Foundation of China under Grant No. 21003056

## Notes and references

[a] *College of Chemistry and State Key Laboratory of Inorganic Synthesis and Preparative Chemistry, Jilin University, Changchun, Jilin, 130023. E-mail:cuixb@mail.jlu.edu.cn.*

[b] *College of Chemistry, Jilin University, Changchun, Jilin, 130023.*

[c] *State Key Laboratory of Urban Water Resource and Environment (SKLUWRE) & Academy of Fundamental and Interdisciplinary Sciences, Harbin Institute of Technology, Harbin, China, 150080*

† Footnotes should appear here. These might include comments relevant to but not central to the matter under discussion, limited experimental and spectral data, and crystallographic data.

Electronic Supplementary Information (ESI) available: [details of any supplementary information available should be included here]. See DOI: 10.1039/b000000x/

1 Citations here in the format A. Name, B. Name and C. Name, *Journal Title*, 2000, **35**, 3523; A. Name, B. Name and C. Name, *Journal Title*, 2000, **35**, 3523.

1. a) M. T. Pope, *Heteropoly and Isopoly Oxometalates*, Springer, Berlin, 1983; b) M. T. Pope and A. Müller, *Angew. Chem., Int. Edit. Engl.*, 1991, **30**, 34; c) M. T. Pope and A. Müller, *Polyoxometalates: From Platonic Solids to Anti-Retro Viral Activity*, Kluwer, Dordrecht, The Netherlands, 1994; d) C. L. Hill, *Chem. Rev.*, 1998, **98**, 1; e) A. Proust, R. Thouvenot and P. Gouzerh, *Chem. Commun.*, 2008, 1837; f) D. L. Long, E. Burkholder and L. Cronin, *Chem. Soc. Rev.*, 2007, 105; g) D. L. Long, R. Tsunashima and L. Cronin, *Angew. Chem. Int. Ed. Engl.*, 2010, **49**, 1736; h) A. Dolbecq, E. Dumas, C. R. Mayer and P. Mialane, *Chem. Rev.*, 2010, **110**, 6009; i) S. Roy, *Crystengcomm.*, 2014, **16**, 4667.
2. a) P. J. Hagrman, D. Hagrman and J. Zubieta, *Angew. Chem. Int. Edit*, 1999, **38**, 2638; b) D. Hagrman, C. Zubieta, D. J. Rose, J. Zubieta and R. C. Haushalter, *Angew. Chem. Int. Edit*, 1997, **36**, 873; c) J. Zubieta, in *Comprehensive coordination chemistry II*, eds. J. A. McCleverty and T. J. Meyer, 2003, p. 697.
3. a) M. I. Khan, E. Yohannes and R. J. Doedens, *Angew. Chem. Int. Ed. Engl.*, 1999, **38**, 1292; b) J. Lu, Y. Xu, N. K. Goh and L. S. Chia, *Chem. Commun.*, 1998, 2733; c) A. Tripathi, T. Hughbanks and A. Clearfield, *J. Am. Chem. Soc.*, 2003, **125**, 10528; d) A. Dolbecq, P. Mialane, L. Lisnard, J. Marrot and F. Sécheresse, *Chem. Eur. J.*, 2003, **9**, 2914; e) P. Mialane, A. Dolbecq and F. Sécheresse, *Chem. Commun.*, 2006, 3477; f) J. Thomas and A. Ramanan, *Cryst. Growth Des.*, 2008, **8**, 3391.
4. a) Y. P. Ren, X. J. Kong, X. Y. Hu, M. Sun, L. S. Long, R. B. Huang and L. S. Zheng, *Inorg. Chem.*, 2006, **45**, 4016; b) G. C. Qu, L. Jiang, X. L. Feng and T. B. Lu, *Dalton Trans.*, 2009, 71; c) S. T. Zheng, J. Zhang and G. Y. Yang, *Angew. Chem. Int. Ed. Engl.*, 2008, **47**, 3909; d) J. W. Zhao, C. M. Wang, J. Zhang, S. T. Zheng and G. Y. Yang, *Chem. Eur. J.*, 2008, **14**, 9223; e) Q. X. Han, X. P. Sun, J. Li, P. T. Ma and J. Y. Niu, *Inorg. Chem.*, 2014, **53**, 6107.
5. a) X. B. Cui, J. Q. Xu, H. Meng, S. T. Zheng and G. Y. Yang, *Inorg. Chem.*, 2004, **43**, 8005; b) L. N. Xiao, Y. Y. Hu, L. M. Wang, Y. Wang, J. N. Xu, H. Ding, X. B. Cui and J. Q. Xu, *Crystengcomm.*, 2012, **14**, 8589; c) L. M. Wang, Y. Wang, Y. Fan, L. N. Xiao, Y. Y. Hu, Z. M. Gao, D. F. Zheng, X. B. Cui and J. Q. Xu, *crystengcomm.*, 2014, **16**, 430; d) H. Y. Guo, Z. F. Li, D. C. Zhao, Y. Y. Hu, L. N. Xiao, X. B. Cui, J. Q. Guan and J. Q. Xu, *Crystengcomm.*, 2014, **16**, 2251; e) L. N. Xiao, J. N. Xu, Y. Y. Hu, L. M. Wang, Y. Wang, H. Ding, X. B. Cui and J. Q. Xu, *Dalton Trans.*, 2013, **42**, 5247.
6. a) F. J. Ma, S. X. Liu, C. Y. Sun, D. D. Liang, G. J. Ren, F. Wei, Y. G. Chen and Z. M. Su, *J. Am. Chem. Soc.*, 2011, **133**, 4178; b) X. L. Wang, D. Zhao, A. X. Tian and J. Ying, *Dalton Trans.*, 2014, **43**, 5211; c) X. L. Wang, N. Han, H. Y. Lin, A. X. Tian, G. C. Liu and J. W. Zhang, *Dalton Trans.*, 2014, **43**, 2052; d) A. X. Tian, J. Ying, J. Peng, J. Q. Sha, Z. M. Su, H. J. Pang, P. P. Zhang, Y. Chen, M. Zhu and Y. Shen, *Cryst. Growth Des.*, 2010, **10**, 1104; e) W. C. Chen, C. Qin, X. L. Wang, Y. G. Li, H. Y. Zang, Y. Q. Jiao, P. Huang, K. Z. Shao, Z. M. Su and E. B. Wang, *Chem. Commun.*, 2014, **50**, 13265; f) J. Q. Shen, Y. Zhang, Z. M. Zhang, Y. G. Li, Y. Q. Gao and E. B. Wang, *Chem. Commun.*, 2014, **50**, 6017; g) M. G. Liu, P. P. Zhang, J. Peng, H. X. Meng, X. Wang, M. Zhu, D. D. Zhang, C. L. Meng and K. Alimaje, *Cryst. Growth Des.*, 2012, **12**, 1273.
7. a) L. Yuan, C. Qin, X. L. Wang, E. B. Wang and S. Chang, *Eur. J. Inorg. Chem.*, 2008, 4936; b) J. Tao, X. M. Zhang, M. L. Tong and X. M. Chen, *J. Chem. Soc., Dalton Trans.*, 2001, 770; c) L. Lisnard, A. Dolbecq, P. Mialane, J. Marrot, E. Codjovi and F. Sécheresse, *Dalton Trans.*, 2005, **24**, 3913; d) H. Jin, Y. F. Qi, E. B. Wang, Y. G. Li, C. Qin, X. L. Wang and S. Chang, *Eur. J. Inorg. Chem.*, 2006, 4541; e) H. Jin, Y. F. Qi, E. B. Wang, Y. G. Li, X. L. Wang, C. Qin and S. Chang, *Cryst. Growth Des.*, 2006, **6**, 2693.
8. a) S. Reinoso, P. Vitoria, L. Lezama, A. Luque and J. M. Gutiérrez-Zorrilla, *Inorg. Chem.*, 2003, **42**, 3709; b) S. Reinoso, P. Vitoria, L. Felices, L. Lezama and J. M. Gutiérrez-Zorrilla, *Inorg. Chem.*, 2006, **45**, 108; c) S. Reinoso, P. Vitoria, J. M. Gutiérrez-Zorrilla, L. Lezama, L. S. Felics and J. I. Beitia, *Inorg. Chem.*, 2005, **44**, 9731; d) X. Y. Zhao, D. D. Liang, S. X. Liu, C. Y. Sun, R. G. Cao, C. Y. Gao, Y. H. Ren and Z. M. Su, *Inorg. Chem.*, 2008, **47**, 7133; e) Y. Yang, S. X. Liu, C. C. Li, S. J. Li, G. J. Ren, F. Wei and Q. Tang, *Inorg. Chem. Commun.*, 2012, **17**, 54; f) Q. X. Han, P. T. Ma, J. W. Zhao, J. P. Wang and J. Y. Niu, *Inorg. Chem. Commun.*, 2011, **14**, 767; g) S. Reinoso, P. Vitoria, L. S. Feilices, L. Lezama and J. M. Gutiérrez-Zorrilla, *chem. Eur. J.*, 2005, **11**, 1538.
9. a) C. Z. Lu, C. D. Wu, H. H. Zhuang and J. S. Huang, *Chem. Mater.*, 2002, **14**, 2649; b) Z. K. Qu, K. Yu, Z. F. Zhao, Z. H. Su, J. Q. Sha, C. M. Wang and B. B. Zhou, *Dalton Trans.*, 2014, **43**, 6744; c) S. W. Zhang, Y. X. Li, Y. Liu, R. G. Cao, C. Y. Sun, H. M. Ji and S. X. Liu, *J. Mol. Struct.*, 2009, **920**, 284; d) X. L. Wang, Q. Gao, G. C. Liu, H. Y. Lin, A. X. Tian and J. Li, *Inorg. Chem. Commun.*, 2011, **14**, 745; e) X. L. Wang, H. L. Hu, A. X. Tian, H. Y. Lin, J. Li and L. M. Shi, *Inorg. Chem. Commun.*, 2010, **13**, 745.
10. a) D. C. Zhao, Y. Y. Hu, H. Ding, H. Y. Guo, X. B. Cui, X. Zhang, Q. S. Huo and J. Q. Xu, *Dalton Trans.*, 2015, **44**, 8971; b) Y. Y. Hu, X. Zhang, D. C. Zhao, H. Y. Guo, L. W. Fu, L. L. Guo, X. B. Cui, Q. S. Huo and J. Q. Xu, *Dalton Trans.*, 2015, **44**, 14830.
11. a) A. Müller and J. Döring, *Angew. Chem. Int. Ed. Engl.*, 1988, **27**, 1721; b) G. Huan, M. A. Greaney and A. J. Jacobson, *j. Chem. Soc., Chem. Commun.*, 1991, 260; c) R. Basler, G. Chaboussant, A. Sieber, H. Andres, M. Murrie, P. Kögerler, H. Bögge, D. C. Crans, E. Krickemeyer, S. Janssen, H. Mutka, A. Müller and H. U. Gudel, *Inorg. Chem.*, 2002, **41**, 5675.
12. G. Sheldrick, *Acta Crystallogr., Sec. A.*, 2008, **64**, 112.
13. L. Farrugia, *J. Appl. Crystallogr.*, 2012, **45**, 849.
14. X. B. Cui, K. C. Li, L. Ye, Y. Chen, J. Q. Xu, W. J. Duan, H. H. Yu, Z. H. Yi and J. W. Cui, *J. Solid. State. Chem*, 2008, **181**, 221.
15. I. D. Brown, *in Structure and Bonding in Crystals, edited by M. O'Keefe, A. Navrotsky*, Academic Press, New York, 1981.
16. N. Masciocchi, G. A. Ardizzoia, G. LaMonica, A. Maspero, S. Galli and A. Sironi, *Inorg. Chem.*, 2001, **40**, 6983.
17. N. Masciocchi, F. Castelli, P. M. Forster, M. M. Tafoya and A. K. Cheetham, *Inorg. Chem.*, 2003, **42**, 6147.
18. a) Y. Xu, J. Q. Xu, K. L. Zhang, Y. Zhang and Y. Z. You, *Chem. Commun.*, 2000, 153; b) J. Y. Niu, Z. L. Wang and J. P. Wang, *inorg. Chem. Commun.*, 2003, **6**, 1272; c) Y. Lu, Y. Xu, E. B. Wang, J. Lü, C. W. Hu and L. Xu, *Cryst. Growth Des.*, 2005, **5**, 257; d) C. M. Liu, D. Q. Zhang and D. B. Zhu, *Cryst. Growth Des.*, 2003, **3**, 363; e) Y. K. Lu, X. B. Cui, Y. B. Liu, Q. F. Yang, S. Y. Shi, J. Q. Xu and T. G. Wang, *J. Solid. State. Chem*, 2009, **182**, 690.
19. a) G. A. Zank, B. Rauchfuss and S. R. Wilson, *J. Am. Chem. Soc.*, 1984, **106**, 7621; b) C. Y. Tang, F. Wang, W. Q. Zhang and D. X. Jia, *Inorg. Chem.*, 2013, **52**, 10860.
20. M. Yuan, Y. G. Li, E. B. Wang, C. G. Tian, L. Wang, C. W. Hu, N. H. Hu and H. Q. Jia, *Inorg. Chem.*, 2003, **42**, 3670.

21. C. M. Liu, D. Q. Zhang, M. Xiong and D. B. Zhu, *Chem. Commun.*, 2002, 1416.
22. T. D. Keene, D. M. D'Alessandro, K. W. Krämer, J. R. Price, D. J. Price, S. Decurtins and C. J. Kepert, *Inorg. Chem.*, 2012, **51**, 9192.
23. H. J. Tian, I. E. Wachs and L. E. Briand, *J. Phys. Chem. B.*, 2005, **109**, 23491.
24. C. L. Wang, G. P. Zhou, Z. B. Zhang, D. R. Zhu and Y. Xu, *J. Coord. Chem.*, 2011, **64**, 1198.

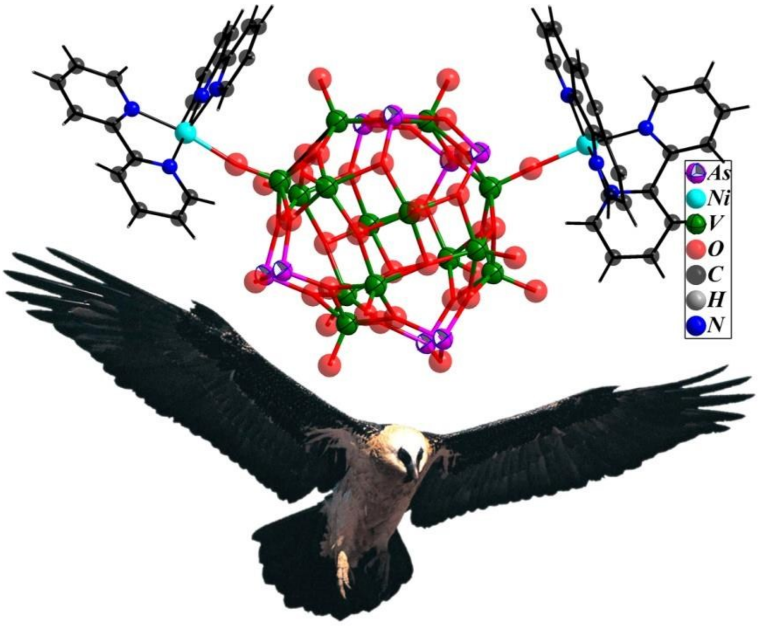

Seven compounds exhibiting novel structures constructed from arsenic-vanadium polyoxoanions and metal mixed-organic-ligand complexes have already been synthesized and characterized.